

# Observation of 99% pump depletion in single-pass second-harmonic generation in a periodically poled lithium niobate waveguide

Krishnan R. Parameswaran, Jonathan R. Kurz, Rostislav V. Roussev, and Martin M. Fejer

*Edward L. Ginzton Laboratory, Stanford University, Stanford, California 94305-4085*

Received August 16, 2001

We report 99% pump depletion in single-pass second-harmonic generation. Quasi-cw pulses at 1550 nm were frequency doubled in an annealed proton-exchanged waveguide formed in periodically poled lithium niobate. Measurements of pump depletion and second-harmonic generation agree with results from numerical integration of the coupled-mode equations that describe the process. © 2002 Optical Society of America

OCIS codes: 190.2620, 190.4360, 190.4410.

Efficient second-harmonic generation (SHG) has many important applications, including novel devices using cascaded  $\chi^{(2)}$  processes<sup>1,2</sup> and quantum optical applications such as squeezed light generation.<sup>3</sup> Achieving pump depletion (which, in lossless systems, is equivalent to energy conversion) greater than 90% in single-pass bulk interactions is challenging.<sup>4,5</sup> The (typically) Gaussian transverse dependence of beam intensity results in nonuniform nonlinear drive, which, together with the attendant narrowing of the acceptance bandwidths, limits the overall conversion efficiency. For example (as discussed in Ref. 6), for an input pulse with a Gaussian profile in space and time, when the maximum local power-conversion efficiency is 99%, the overall energy-conversion efficiency (i.e., the local instantaneous efficiency averaged over time and radial coordinates) is only 75%. To increase energy conversion to 99% in a device of fixed length, one would have to increase the peak power more than 40 times beyond this point. At these drive levels, severe issues of backconversion, gain-induced diffraction, and in many cases surface damage, would occur. Quadrature frequency conversion<sup>7</sup> is a technique that has been used to get more than 95% energy conversion by use of two crystals of different lengths to address separately the high- and low-intensity portions of the pump beam, generating harmonic waves that are orthogonally polarized in the two regions. This approach is somewhat complicated and generates output with transverse variations in the polarization state.

Quasi-cw interactions in a guided-wave configuration circumvent these problems. Transverse variations in the mixing efficiency and diffraction effects are eliminated, since the waveguide modes interact as entities. Normalized conversion efficiencies are also much higher than in the bulk case because of the two-dimensional spatial confinement provided by the waveguide; this reduces the power required for strong pump depletion, thereby opening up the choice of pump lasers to include quasi-cw and even cw sources.

The electric field profiles in a waveguide can be described by the product of an envelope function that evolves with position and a position-independent transverse profile:  $E_\omega(x, y, z) = A_\omega(z)E_\omega(x, y)\exp(-jk_\omega z)$  and  $E_{2\omega}(x, y, z) = A_{2\omega}(z)E_{2\omega}(x, y)\exp(-jk_{2\omega} z)$ . The transverse profile,  $E(x, y)$ , is an eigenmode whose

shape is determined by the index profile of the waveguide. The evolution of the envelopes during SHG in guided-wave structures can be described by the following coupled-mode equations:

$$\frac{dA_\omega}{dz} = -j\sqrt{\eta_0}A_\omega^*A_{2\omega}\exp(-j\Delta kz) - \alpha_\omega A_\omega, \quad (1a)$$

$$\frac{dA_{2\omega}}{dz} = -j\sqrt{\eta_0}A_\omega^2\exp(-j\Delta kz) - \alpha_{2\omega}A_{2\omega}, \quad (1b)$$

where the normalized efficiency  $\eta_0$  [1/W cm<sup>2</sup>] is proportional to the square of the effective nonlinear coefficient and the spatial overlap of the transverse modes at the two wavelengths in the waveguide,  $\alpha$  [cm<sup>-1</sup>], is the field propagation loss coefficient, and  $\Delta k$  [cm<sup>-1</sup>] is the phase mismatch,  $k_2 - 2k_1$ , where  $k_i$  are the modal propagation constants. The envelopes are normalized such that the power in each wave  $P_i = |A_i|^2$ . When  $\Delta k = 0$  as the second harmonic grows from the input of the guide, its phase relative to the fundamental is locked at  $\pi/2$ , such that power flows unidirectionally from the fundamental to the second-harmonic wave. If the device is lossless, the solution is well known:

$$\eta \equiv \frac{P_{2\omega}(z)}{P_\omega(0)} = \tanh^2[(\eta_0 P_\omega(0) z^2)^{1/2}] = \tanh^2(\Gamma z), \quad (2)$$

where we define the nonlinear drive as  $\Gamma = \sqrt{\eta_0 P_\omega(0)}$ . It is the slow approach of  $\eta$  to unity with increasing  $P_\omega$  that leads to the difficulties associated with the very strong peak drive required for the energy-conversion efficiency (or pump depletion) to be brought close to unity.

Parasitic processes can limit the observable pump depletion in the large-conversion regime. The coupled-mode equations describing near-degenerate parametric amplification of signal and idler fields close to the pump frequency in a lossless waveguide are

$$\frac{dA_s}{dz} = -j\sqrt{\eta_0}A_{2\omega}A_i^*, \quad (3a)$$

$$\frac{dA_i}{dz} = -j\sqrt{\eta_0}A_{2\omega}A_s^*, \quad (3b)$$

where  $\omega_s + \omega_i = 2\omega$ , and we take  $\Delta k = k_{2\omega} - k_s - k_i = 0$ . Using Eq. (2) for evolution of the second-harmonic field, we find that the solution for the parametric gain in the undepleted pump limit is

$$G = \left| \frac{A_i(L)}{A_s(0)} \right|^2 = \frac{\eta^2}{4(1-\eta)}. \quad (4)$$

When  $\eta = 0.99$ ,  $G = 14$  dB, so small amounts of amplified spontaneous emission at the device input (as might be present, for example, from an amplified cw pump laser) can be parametrically amplified, converting power back to the pump band, limiting the observable level of pump depletion. At this level of parametric gain, one must also suppress feedback from facet reflections to avoid parametric oscillation, as the 14% reflection characteristic of a  $90^\circ$  facet in a periodically poled lithium niobate (PPLN) waveguide is sufficient to reach oscillation threshold.<sup>7</sup> These problems can be largely mitigated by narrow-band filtering of the pump source and angle polishing of the end faces, respectively.

One difficulty in the large-depletion regime that is not easily avoided is that of narrowing of the phase-matching bandwidth. The exact solution to the coupled-mode equations that describe plane-wave SHG (or SHG with single waveguide modes) in a lossless medium of length  $L$  is<sup>6</sup>

$$\eta = \frac{I_{2\omega}(L)}{I_\omega(0)} = \nu_b^2 \operatorname{sn}^2\left(\frac{\Gamma L}{\nu_b}, \nu_b^4\right), \quad (5)$$

where

$$\nu_b = \frac{1}{\Delta k/4\Gamma + [1 + (\Delta k/4\Gamma)^2]^{1/2}}, \quad (6)$$

and  $\operatorname{sn}$  is a Jacobi elliptic function. At low  $\Gamma$  (corresponding to low conversion efficiency) the function simplifies to the familiar  $\operatorname{sinc}^2(\Delta kL)$ . The solution simplifies to the  $\tanh^2$  form given in Eq. (2) for  $\Delta k = 0$ , whereas for arbitrary  $\Delta k$ , the peak conversion efficiency asymptotically approaches unity and the width of the main lobe of the Jacobi elliptic function rapidly narrows with increasing  $\Gamma L$ . Figure 1 shows that when the conversion efficiency reaches 99% (at  $\Gamma L = 3$ ), the FWHM of the main lobe drops to  $\sim 30\%$  of its low-power value. For a 6-cm-long annealed proton-exchanged waveguide in periodically poled lithium niobate operating near 1550 nm, this corresponds to a drop from 0.17 to 0.052 nm in wavelength space, with corresponding drops in acceptance for temperature variations and for axial inhomogeneities in the waveguide structure.

The presence of propagation losses precludes analytical solution of Eqs. (1a) and (1b) but leaves the essential conclusions of the discussion above unchanged. To clarify contributions of linear and nonlinear effects in analyzing experimental data, it is useful to compare the transmission at low and high pump powers ( $T_\omega[P_\omega(0) \approx 0]$  and  $T_\omega[P_\omega(0)]$ , respectively), where for

a device of length  $L$ , we define the transmission at the fundamental wavelength as  $T_\omega \equiv P_\omega(L)/P_\omega(0)$ , such that the pump depletion becomes

$$D[P_\omega(0)] \equiv 1 - \frac{T_\omega[P_\omega(0)]}{T_\omega[P_\omega(0) \approx 0]}, \quad (7)$$

which is readily computed by straightforward numerical integration of Eqs. (1a) and (1b). For a phase-matched interaction, the pump depletion asymptotically approaches unity with increasing pump power.

Device fabrication involved electric field poling<sup>8</sup> of a 7.62-cm-diameter lithium niobate wafer with a quasi-phase-matching period of 14.74  $\mu\text{m}$ . The waveguide width in the mixing region was 12  $\mu\text{m}$ , with an initial proton-exchange depth of 0.71  $\mu\text{m}$  and annealing time of 26 h at 328  $^\circ\text{C}$ . Mode filters and tapers were used to facilitate launching into the fundamental transverse mode of the waveguide.<sup>9</sup> The total sample length was 6.45 cm, and the end faces were polished at a  $6^\circ$  angle.

Figure 2 shows a low-power, cw SHG tuning curve for the waveguide used in this experiment. We define the conversion efficiency as  $\eta_{\text{meas}} \equiv P_{2\omega}(L)/[P_\omega(L)]^2$ , such that both powers are measured at the waveguide output. The theoretical calculation used typical values of power propagation losses,  $2\alpha$ , at the fundamental and the second-harmonic wavelengths (0.43 and 0.59 dB/cm, respectively). The peak efficiency of the calculated curve is chosen such that the areas under the measured and calculated curves are equal, which results in a value of  $\eta_0 = 38.0\%/W \text{ cm}^2$ . The slight deviation of the measurement from the calculation is caused by residual phase mismatch along the length of the device, which arises from imperfections in the fabrication process.

The experimental setup used in the pump-depletion experiment is identical to that described in Ref. 10, in which three erbium-doped fiber amplifiers and

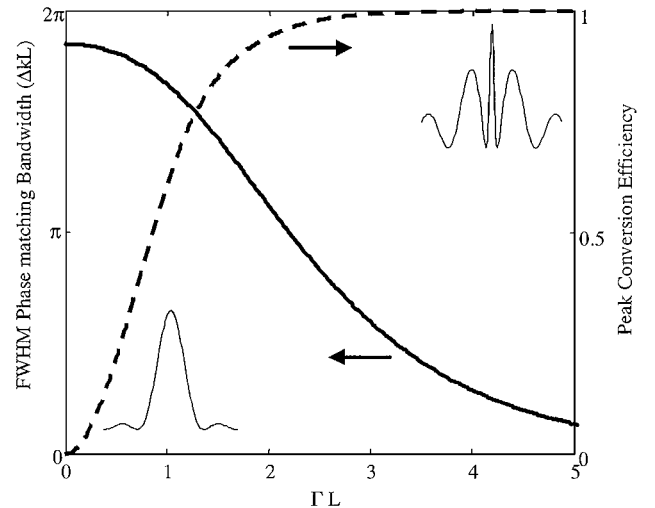


Fig. 1. Calculated FWHM (solid curve) and peak conversion efficiency (dashed curve) as functions of normalized input pump power. The insets show wavelength-tuning curves at low (left) and high (right) conversion efficiency.

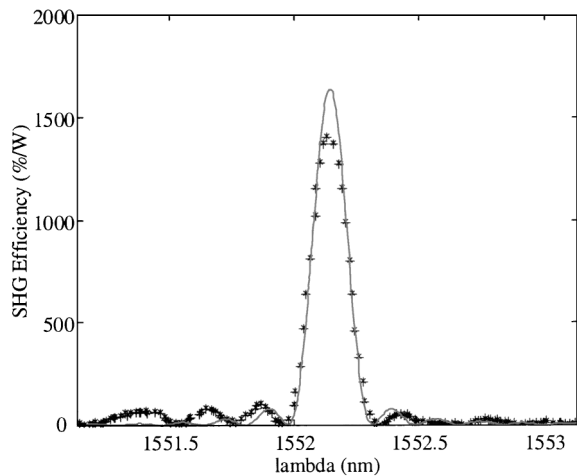


Fig. 2. Measured low-power cw SHG tuning curve and calculation for an axially uniform waveguide with losses of  $2\alpha_{\omega} = 0.43$  dB/cm and  $2\alpha_{2\omega} = 0.59$  dB/cm. The peak conversion efficiency is  $\eta = 1400\%/W$ .

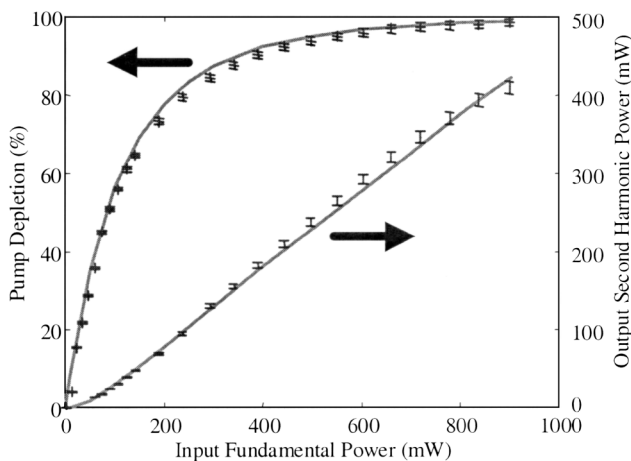


Fig. 3. Measured and calculated pump depletion and output second harmonic versus input power. Pump depletion of 99% is observed at an input power of 900 mW. All powers are peak values.

an electro-optic amplitude modulator are used to produce watt-level quasi-cw pulses from a tunable cw external-cavity diode laser. The laser linewidth is less than 5 MHz, where the external modulator produces 50-ns pulses at a 1-kHz repetition rate. With this pulse width and the 6.45-cm sample length, group-velocity walk-off is negligible. A narrow-band (0.1-nm FWHM) fiber Bragg grating and circulator are used to limit the amplified spontaneous emission power launched into the waveguide. The experiment was done at room temperature.

Figure 3 shows a plot of pump depletion as a function of pump power launched into the waveguide, along with a calculation with the same values of propagation losses and normalized efficiency as those used in the low-power fit. The three signals (fundamental in, fundamental out, second-harmonic out) were measured by time resolution of the pulses detected by calibrated photodiodes on a digital oscilloscope, such that

all powers are peak values. Good agreement with theory is observed, with pump depletion reaching 99% at an input power near 900 mW. A plot of the generated power at the second-harmonic wavelength is also shown in Fig. 3, where again agreement is very good. When the input power is increased beyond this point, the curves turn around. The small residual phase mismatch that is apparent from the cw tuning curve may be the source of this phenomenon. Parametric amplification of residual amplified spontaneous emission from the amplifiers by the strong second-harmonic signal is another possibility.

One can improve the conversion efficiency by reducing the propagation losses and increasing the modal overlap. Using the reverse proton-exchange process<sup>11</sup> to create a more-symmetric index profile in depth, Parameswaran *et al.* recently observed a fourfold improvement in normalized conversion efficiency, to  $150\%/W\text{ cm}^2$ ,<sup>12</sup> which would reduce the pump power for reaching the same depletion observed here from 900 to 225 mW. In future work we will explore the use of these highly nonlinear waveguides in high-gain parametric devices for applications in optical communications and quantum optics.

This work was supported by the Defense Advanced Research Projects Agency through the Optoelectronics Materials Center, by the National Science Foundation through contract ECS-9903156, and by the U.S. Air Force Office of Scientific Research through contract 49620-99-1-0270. K. Parameswaran's e-mail address is krishp@stanford.edu.

## References

1. M. H. Chou, K. R. Parameswaran, I. Brener, and M. M. Fejer, *IEICE Trans. Electron.* **E83C**, 869–874 (2000).
2. K. Gallo and G. Assanto, *J. Opt. Soc. Am. B* **16**, 267–269 (1999).
3. R.-D. Li and P. Kumar, *Phys. Rev. A* **49**, 2157–2166 (1994).
4. D. Eimerl, *IEEE J. Quantum Electron.* **QE-23**, 575–592 (1987).
5. D. Taverner, P. Britton, P. G. R. Smith, D. J. Richardson, G. W. Ross, and D. C. Hanna, *Opt. Lett.* **23**, 162–164 (1998).
6. R. C. Eckardt and J. Reintjes, *IEEE J. Quantum Electron.* **20**, 1178–1187 (1984).
7. D. Eimerl, *IEEE J. Quantum Electron.* **QE-23**, 1361–1371 (1987).
8. L. E. Myers, R. C. Eckardt, M. M. Fejer, R. L. Byer, W. R. Bosenberg, and J. W. Pierce, *J. Opt. Soc. Am. B* **12**, 2102–2116 (1995).
9. M. H. Chou, I. Brener, M. M. Fejer, E. E. Chaban, and S. B. Christman, *IEEE Photon. Technol. Lett.* **11**, 653–655 (1999).
10. K. Gallo, G. Assanto, K. R. Parameswaran, and M. M. Fejer, *Appl. Phys. Lett.* **79**, 314–316 (2001).
11. Yu. N. Korkishko, V. A. Fedorov, T. M. Morozova, F. Caccavale, F. Gonella, and F. Segato, *J. Opt. Soc. Am. A* **15**, 1838–1842 (1998).
12. K. R. Parameswaran, R. K. Route, J. R. Kurz, R. V. Roussev, M. M. Fejer, and M. Fujimura, in *LEOS 2001 Annual Meeting* (Lasers and Electro-Optics Society, Piscataway, N.J., 2001), paper ThL 3.